EXPERIMENTS WITH A FAST CHOPPER SYSTEM FOR INTENSE ION BEAMS

H. Dinter[*], M. Droba, M. Lotz, O. Meusel, I. Mueller, D. Noll, U. Ratzinger, K. Schulte, C. Wagner, C. Wiesner, Institute for Applied Physics (IAP), Goethe-University, Frankfurt am Main, Germany

Abstract

Chopper systems are used to pulse charged particle beams. In most cases, electric deflection systems are used to generate beam pulses of defined lengths and appropriate repetition rates. At high beam intensities, the field distribution of the chopper system needs to be adapted precisely to the beam dynamics in order to avoid aberrations [1]. An additional challenge is a robust design which guarantees reliable operation.

For the Frankfurt Neutron Source FRANZ [2], an $E \times B$ chopper system [1] is being developed which combines static magnetic deflection with a pulsed electric field in a Wien filter configuration. It will generate proton pulses with a flat top of 50 ns at a repetition rate of 250 kHz for 120 keV, 200 mA beams. For the electric deflection, pre-experiments with static and pulsed fields were performed [3] using a helium ion beam. In pulsed mode operation, ion beams of different energies were deflected with voltages of up to ± 6 kV and the resulting response was measured using a beam current transformer. A comparison between experiments and theoretical calculations as well as numerical simulations are presented.

INTRODUCTION
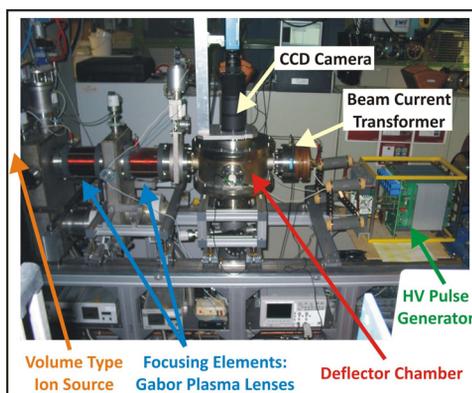
Figure 1: Components of the deflector test stand.

Fast electric chopper systems pose a great challenge in their technical realisation. They often suffer from sputtering, deterioration of insulators and high voltage breakdowns [4]. These effects become even more critical for high intensity ion beams with currents of several mA. It is thus important to examine the behaviour of chopper sys-

tems under realistic conditions. For this purpose, a deflector test stand for high intensity ion beams shown in Fig. 1 was installed.

In the deflector chamber, helium beams up to 25 keV, 1 mA were deflected between two copper plates of 15 cm length with an aperture of 7.6 cm [3]. For static beam deflection, voltage was applied to one plate, the other plate being grounded. In pulsed mode operation, both plates were oppositely charged with symmetric voltages provided by a high voltage pulse generator.

BEAM TRANSPORT SIMULATIONS

The BENDER simulation package [5] is currently under development. This toolkit is capable of transporting single particles and particle distributions in external electric and magnetic fields considering space charge forces using the Particle-In-Cell (PIC) method. External fields are generated from an analytic description or imported from different sources, e.g. ASCII files, or from CST Suite.

The settings of the experiments were simulated and the results were compared to the measurements by tracking particles through the field distribution of the deflector system for different field intensities. The resulting beam profiles and deflection angles were evaluated. As particle input, a measured beam distribution behind the ion source was used. The electric field was calculated using CST EM Studio (EMS).

STATIC BEAM DEFLECTION
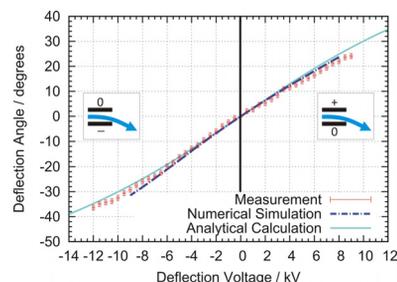
Figure 2: Static deflection angle for $U_B = 20$ kV [1]. To eliminate influences of the plate geometry on the deflection angle, the beam was always bent towards the right plate by swapping charged and grounded plate for negative voltages.

For an ion beam accelerated longitudinally by U_B, the deflection angle induced by a transverse electric field, cre-

[*] dinter@iap.uni-frankfurt.de

05 Beam Dynamics and Electromagnetic Fields

D04 High Intensity in Linear Accelerators

ated between two plates of distance d and deflection voltage U, is given by [3]

$$\alpha = \tan^{-1}\left(\frac{1}{2}\frac{l_{\text{eff}}}{d}\frac{U}{U_B}\right) \ , \ l_{\text{eff}} = \frac{d}{U}\int_{-\infty}^{\infty} E_x(z)\,\mathrm{d}z \quad (1)$$

with the effective length l_{eff} of an equivalent constant field.

Deflection angles were measured using the CCD camera mounted above the deflector chamber. The voltage-angle dependency (Fig. 2) shows good agreement with the particle simulations and analytical calculations. For high deflection voltages, the beam passes the deflector plates at a very short distance which leads to differences between simulation, experiment and analytical model.

Current Flow to Deflector Plates

Along with the beam profile and deflection angle, the current flow to the deflector plates as well as the residual gas pressure in the vacuum chamber were measured. In Fig. 3, four voltage regions of characteristic behaviour can be distinguished.
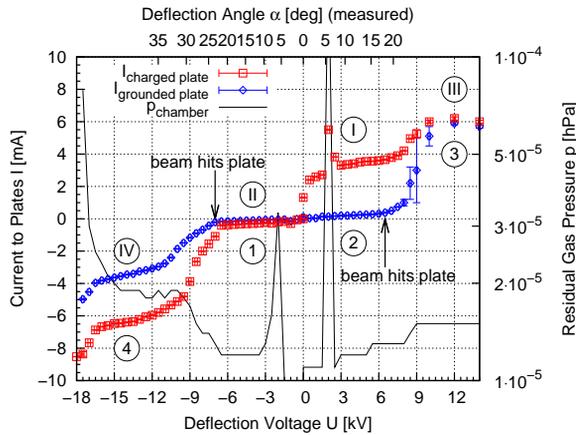
Figure 3: Electric current to deflector plates and residual gas pressure plotted against voltage for $U_B = 20\,\text{kV}$.

For positive deflection voltages, space charge compensation electrons are pulled out of the beam which leads to a current increase on the positive plate (I). As the electrons are not attracted by negative potential, this does not happen for negative voltages (1). For higher deflection angles, the distance between the beam and the plate decreases, more beam halo particles and residual gas ions hit the plate and the current increases slightly (II, 2).

For high deflection voltages, beam ions impact the plate and create numerous secondary electrons (3, 4). At positive voltages, these electrons are pulled towards the positive plate resulting in a current increase (III). In the negative case, only some of the secondary electrons hit the opposite (grounded) plate leading to a lower current (IV) compared to (III).

The beam hitting the plate leads to desorption of gas molecules from the plate surface. Thus, the residual gas pressure increases significantly at high voltages. The same

explanation applies for the peaks at deflection voltages of $\pm 2.0\,\text{kV}$, where the beam grazes the beam pipe at the exit of the deflector chamber under a very small angle and causes desorption in a large area.

Beam Profiles
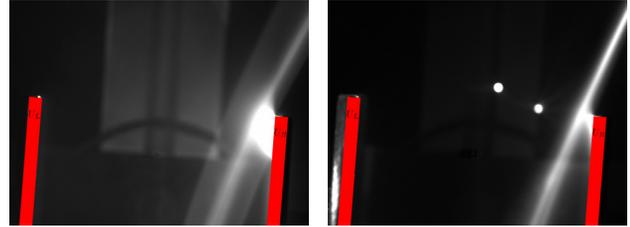
Figure 4: For negative deflection voltages, a halo structure is visible (20 keV beam travelling upwards). **Left:** $U_L = 0\,\text{kV}$, $U_R = -7.5\,\text{kV}$. **Right:** $U_L = +7.5\,\text{kV}$, $U_R = 0\,\text{kV}$.
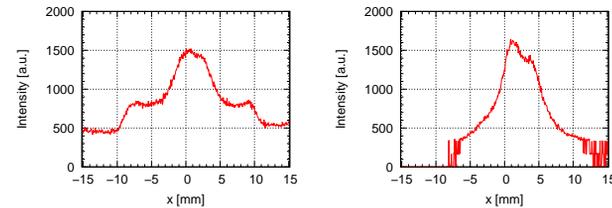
Figure 5: Profiles of the beams shown in Fig. 4.

The potential on the deflection plates has a strong impact on beam transport. This leads to the development of a halo structure for negative voltages (in the left subimage of Fig. 4 and 5). Due to the greater beam width, the current rise in Fig. 3 is slower for negative deflection voltages than for positive ones.
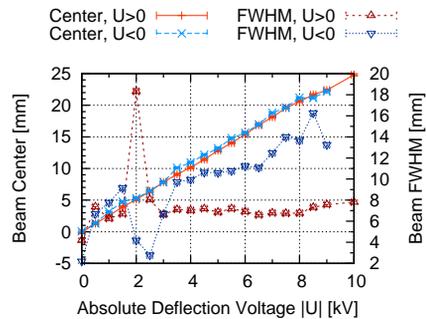
Figure 6: Measured beam center and FWHM width.

To allow for a quantitative characterisation of beam profile and width, the maximum luminance position (beam center) and full-width-half-maximum (FWHM) were calculated from the camera images. The beam center motion in Fig. 6 corresponds to the deflection angle in Fig. 2. The FWHM is larger for negative voltages.

05 Beam Dynamics and Electromagnetic Fields

D04 High Intensity in Linear Accelerators

PULSED MODE OPERATION

Symmetric deflection pulses with repetition rate of 250 kHz and amplitudes up to ± 6 kV were applied to the positive and the negative deflector plate, respectively. Pulse and resulting beam structure were analysed using a fast beam current transformer (BCT).
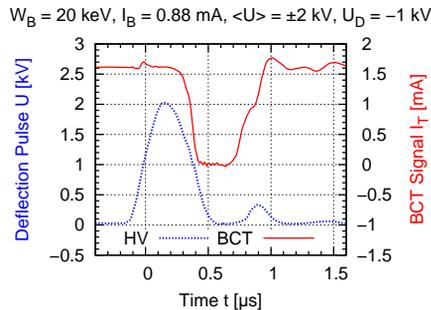
Figure 7: Deflection pulse (lower curve, only positive voltage shown) and BCT response (upper curve).

The main deflector pulse in Fig. 7 is followed by a post-pulse which has no effect on the beam as it is very small. It might however influence electrons in the system which could lead to additional signals in the BCT. To eliminate effects of RF sent from the plates to the BCT, the signal without beam (RF only) was subtracted from the measured data.

The resulting signal in Fig. 7 shows the beam leaving the BCT aperture for a duration of 0.3 ns. Due to the finite beam radius, the edges in the BCT signal are not vertical, but extend over a few nanoseconds. The beam leaves the BCT between 0.3 ns and 0.4 ns and re-enters it between 0.7 ns and 1.0 ns.

When applying a potential to the beam dump, the beam signal changes notably. This is due to the time dependency of space charge compensation conditions. Electrons passing the BCT from various directions at different times overlay with the beam signal. It is planned to perform additional particle simulations and measurements considering time-dependent space charge compensation and secondary electron effects.

Time-Of-Flight Measurements

The flight time of the ions from the plates to the BCT can be measured by observing the delay between the peak in the deflector pulse and the center of the beam pulse plateau. This was done for helium beams with energies between 12 keV and 25 keV over a flight distance of 38.3 cm.

The measured data in Fig. 8 lie slightly above the analytical curve. Possible explanations include uncertainty in the flight distance due to the deflector field not being totally symmetric around the deflector plates and variation of beam energy due to the potential between the plates.
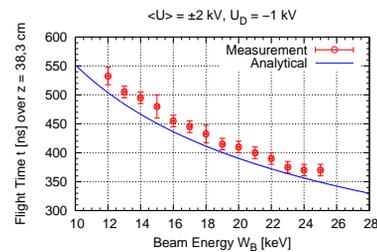
Figure 8: Time-Of-Flight measurements.

CONCLUSION

The behaviour of a fast chopper system for intense ion beams was investigated under realistic conditions. Helium beams of up to 25 keV, 1 mA were deflected with static and pulsed electric fields. In the static case, deflection angles of $38°$ were achieved. In pulsed mode operation, the beam was chopped using 12 kV, 250 kHz pulses. The deflection angle and Time-Of-Flight measurements are in good agreement with analytical calculations and numerical simulations done with the new simulation tool BENDER.

It was observed that beam focusing depends on the deflection voltage and space charge compensation level. The focusing elements however cannot be adjusted in real-time at 250 kHz frequency. To overcome this limitation and avoid further space charge compensation issues, such as current flow to the deflector plates, sputtering and release of secondary particles, the present FRANZ chopper design includes an electric repeller field which keeps compensation electrons out of the deflector chamber and stabilises the space charge state of the beam.

After 250 hours of beam time, insulators of the plate mounting were coated with a metal layer from the chamber wall and plates. It is thus important to protect insulators from sputtering to extend the life time of the system. This can be done by changing the insulator geometry, improving beam dynamics and using materials with a lower sputter yield.

REFERENCES

[1] C. Wiesner et al., "E×B Chopper System for High Intensity Proton Beams", LINAC2010, Tsukuba, 2010, THP071, p. 914 (2010).

[2] C. Wiesner et al., "Proton Driver Linac for the Frankfurt Neutron Source", AIP Conf. Proc. 1265, p. 487 (2010).

[3] H. Dinter, "Experimente mit einem schnellen Choppersystem für intensive Ionenstrahlen", Bachelor Thesis, Frankfurt, 2010.

[4] S-H. Kim and J. Galambos, "High Power Operational Experience at Spallation Neutron Source (SNS)", Proceedings of Technology and Components of Accelerator-driven Systems, Karlsruhe, March 2010.

[5] D. Noll, "Strahldynamische Rechnungen und Kavitätendesign für den FRANZ-Bunchkompressor", Master Thesis, Frankfurt, 2011.

05 Beam Dynamics and Electromagnetic Fields

D04 High Intensity in Linear Accelerators